

**Large magnetic entropy change associated with the weakly first-order paramagnetic to ferrimagnetic transition in antiperovskite manganese nitride CuNMn<sub>3</sub>**

C. Yang, P. Tong, J. C. Lin, S. Lin, D. P. Cui, B. S. Wang, W. H. Song, W. J. Lu, and Y. P. Sun

Citation: *Journal of Applied Physics* **116**, 033902 (2014); doi: 10.1063/1.4890223

View online: <http://dx.doi.org/10.1063/1.4890223>

View Table of Contents: <http://scitation.aip.org/content/aip/journal/jap/116/3?ver=pdfcov>

Published by the **AIP Publishing**

---

**Articles you may be interested in**

[Phase diagram and magnetocaloric effects in Ni<sub>1-x</sub>CrxMnGe<sub>1.05</sub>](#)

*J. Appl. Phys.* **117**, 17A711 (2015); 10.1063/1.4907765

[Observation of the large magnetocaloric effect and suppression of orbital entropy change in Fe-doped MnV<sub>2</sub>O<sub>4</sub>](#)

*J. Appl. Phys.* **115**, 034903 (2014); 10.1063/1.4861630

[Observation of the large orbital entropy in Zn-doped orbital-spin-coupled system MnV<sub>2</sub>O<sub>4</sub>](#)

*Appl. Phys. Lett.* **96**, 062506 (2010); 10.1063/1.3303982

[Entropy determinations and magnetocaloric parameters in systems with first-order transitions: Study of MnAs](#)

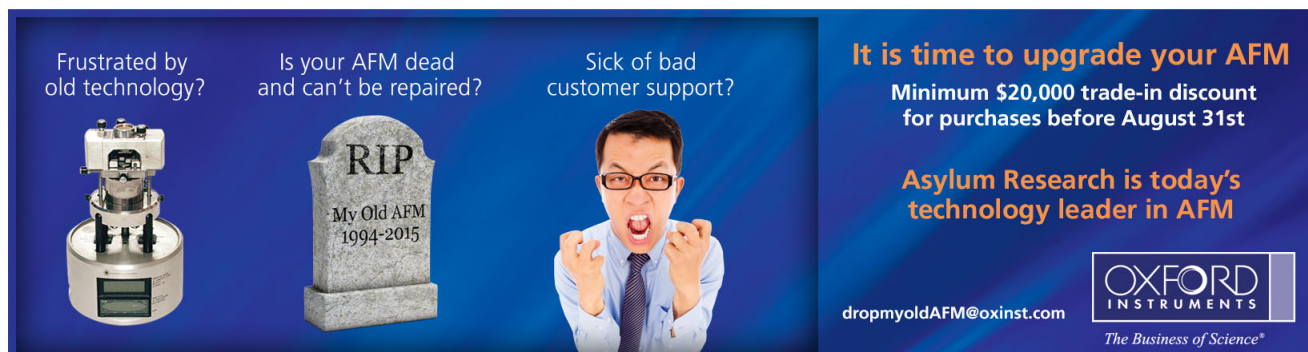
*J. Appl. Phys.* **105**, 093918 (2009); 10.1063/1.3093880

[Manipulation of the metamagnetic transition and entropy change in Gd<sub>5</sub>\(Si,Ge\)<sub>4</sub>](#)

*J. Appl. Phys.* **95**, 6912 (2004); 10.1063/1.1688572

---

Frustrated by old technology?      Is your AFM dead and can't be repaired?      Sick of bad customer support?



**It is time to upgrade your AFM**  
Minimum \$20,000 trade-in discount for purchases before August 31st

**Asylum Research is today's technology leader in AFM**

[dropmyoldAFM@oxinst.com](mailto:dropmyoldAFM@oxinst.com)

**OXFORD INSTRUMENTS**  
The Business of Science®

# Large magnetic entropy change associated with the weakly first-order paramagnetic to ferrimagnetic transition in antiperovskite manganese nitride $\text{CuNMn}_3$

C. Yang,<sup>1</sup> P. Tong,<sup>1,a)</sup> J. C. Lin,<sup>1</sup> S. Lin,<sup>1</sup> D. P. Cui,<sup>1</sup> B. S. Wang,<sup>1</sup> W. H. Song,<sup>1</sup> W. J. Lu,<sup>1</sup> and Y. P. Sun<sup>1,2,3,b)</sup>

<sup>1</sup>Key Laboratory of Materials Physics, Institute of Solid State Physics, Chinese Academy of Sciences, Hefei 230031, People's Republic of China

<sup>2</sup>High Magnetic Field Laboratory, Chinese Academy of Sciences, Hefei 230031, People's Republic of China

<sup>3</sup>University of Science and Technology of China, Hefei 230026, People's Republic of China

(Received 22 April 2014; accepted 1 July 2014; published online 15 July 2014)

We report a systematic study of the specific heat and *dc* magnetic susceptibility on the paramagnetic to ferrimagnetic transition ( $T_C \sim 141$  K) in  $\text{CuNMn}_3$ . A large magnetocaloric effect (MCE) at  $T_C$  is observed with the entropy change of 3.49 J/kg K (6.38 J/kg K) for the field change of  $\Delta H = 20$  kOe (45 kOe). The analysis of the isothermal magnetizations, including the derived Arrott plots and magnetic entropy change, shows a second-order like transition at  $T_C$ . However, the existence of latent heat around  $T_C$  is unambiguously manifested by the reduced slope of the temperature-time relaxations recorded during the specific heat measurement, indicating the transition is in fact weakly first-order in nature. The large MCE comparable with those observed the antiperovskite manganese carbides suggests it is equivalently interesting to explore the MCE in the antiperovskite manganese nitrides as in the carbides. © 2014 AIP Publishing LLC.

[<http://dx.doi.org/10.1063/1.4890223>]

## I. INTRODUCTION

The manganese antiperovskite  $\text{AXMn}_3$  (X: metal or semiconducting elements; X: C or N) compounds have attracted considerable attentions because of their multi-functionalities,<sup>1</sup> such as negative thermal expansion (NTE) or zero thermal expansion (ZTE),<sup>2–5</sup> nearly zero temperature coefficient of resistance (TCR),<sup>6–8</sup> giant magnetoresistance (GMR),<sup>9–11</sup> large magnetocaloric effect (MCE),<sup>12–15</sup> giant magnetostriction (MS),<sup>16</sup> and ferromagnetic (FM) shape memory (FSM) effect.<sup>17</sup>  $\text{CuNMn}_3$  that acts as a parent for studying various functionalities has received significant interest recently. The compound undergoes a high-temperature paramagnetic (PM) to low-temperature ferrimagnetic (FIM) transition at  $T_C \sim 143$  K. Accompanying the PM-FIM transition is a cubic to tetragonal structural transformation without volume change.<sup>6</sup> Above  $T_C$ , the resistivity shows a weak temperature dependence,<sup>6</sup> based on which extremely low TCRs were achieved by element chemical doping.<sup>18</sup> Below  $T_C$ , large MS and FSM effects were observed as well.<sup>16,17</sup> By manipulating the chemical constituents in doped  $\text{CuNMn}_3$ , NTE or ZTE was obtained in various temperature regions.<sup>2–4,19</sup> The ZTE and NTE have been suggested to be related with the broadening of magnetic/lattice transitions.<sup>1,2</sup> A deep investigation on the nature of the PM-FIM transition in  $\text{CuNMn}_3$  would be helpful to better comprehend the mechanisms of the multi-functionalities.

The MCE in the antiperovskite manganese carbides has been extensively studied, while little concern has been paid to that in the nitrides. Here, we report the MCE around  $T_C$  in

$\text{CuNMn}_3$ . A large magnetic entropy change of 6.38 J/kg K was observed with the magnetic field change of 0–45 kOe, which is comparable with those observed in the antiperovskite manganese carbides. The PM-FIM transition looks like a continuous one due to the invisible metamagnetic transition, positive slope in the Arrott plots, and the symmetric change of magnetic entropy under magnetic field. Nevertheless, the delicate analysis the temperature-time relaxations recorded during the specific heat measurement demonstrates that the transition is weakly first-order in nature.

## II. EXPERIMENTS

Polycrystalline sample of  $\text{CuNMn}_3$  was prepared from powders of Cu (4N), Mn (4N), and homemade  $\text{Mn}_2\text{N}$ . The detailed preparation has been reported elsewhere.<sup>18</sup> The specific heat measurements were carried out with a Quantum Design (QD) Physical Property Measurement System (PPMS) ( $2 \text{ K} \leq T \leq 400 \text{ K}$ ,  $0 \leq H \leq 90 \text{ kOe}$ ). The magnetic measurements were performed on a QD superconducting quantum interference device (SQUID) magnetometer ( $1.8 \text{ K} \leq T \leq 400 \text{ K}$ ,  $0 \leq H \leq 50 \text{ kOe}$ ).

## III. RESULTS AND DISCUSSION

Figure 1 shows the temperature dependent magnetization  $M(T)$  of  $\text{CuNMn}_3$  measured at  $H = 100$  Oe under both zero-field-cooled (ZFC) and field-cooled (FC) modes. The magnetic transition temperature derived from the reflection point of derivative of  $M(T)$  curve is about 141 K, which agrees with the result of Ref. 6. Probably because the spins are ferrimagnetically ordered, the ZFC and FC  $M(T)$ s below

<sup>a)</sup>E-mail: tongpeng@issp.ac.cn

<sup>b)</sup>E-mail: ypsun@issp.ac.cn

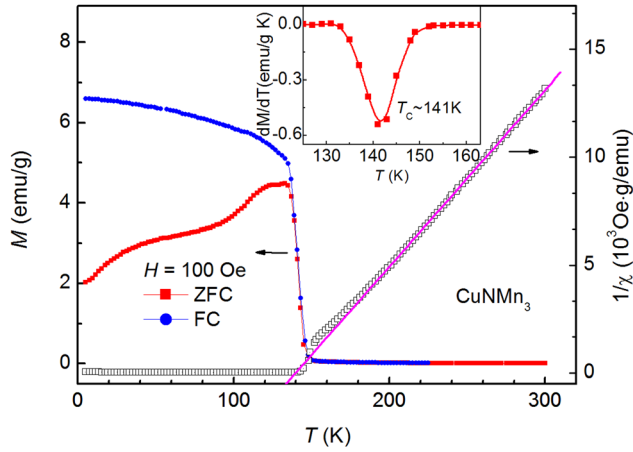


FIG. 1. The field dependent magnetization  $M(T)$  for  $\text{CuNMn}_3$  measured under both ZFC and FC modes. Also shown is the inverse susceptibility  $1/\chi(T)$  deduced from ZFC  $M(T)$ . The solid line is a linear fit to the  $1/\chi(T)$  data following the Curie-Weiss law above  $T_c$ . Inset shows the  $dM/dT$  vs  $T$  curve around  $T_c$ .

$T_c$  show a clear bifurcation. Similar behavior has been observed in  $\text{SnCMn}_3$  which has the same noncollinear magnetic structure as  $\text{CuNMn}_3$ .<sup>20</sup> In the transition area, ZFC curve agrees well with the FC curve, indicating a good thermal reversibility. As shown in Fig. 1, the inverse magnetic susceptibility  $1/\chi(T)$  at high temperatures can be well described by the Curie-Weiss law,  $\chi(T)^{-1} = (T - \theta)/C$ , where  $C$  is the Curie constant,  $\theta$  stands for the Weiss temperature. By fitting the data to the Curie-Weiss law, we get the values of parameters as follows:  $C = 2.948 \text{ emu}\cdot\text{K}/\text{mol}$ ,  $\theta = 140.8 \text{ K}$ . The Weiss temperature is virtually close to the  $T_c$  determined from the  $dM(T)/dT$  curve. The positive  $\theta$  indicates the magnetic interactions are predominantly FM type. The effective magnetic moment per Mn atom,  $\mu_{\text{eff}}$ , is estimated as  $2.81 \mu_B$  from the relationship  $\mu_{\text{eff}} = 2.828(C/\eta)^{1/2} \mu_B$  (where  $\eta$  is the number of magnetic atoms in a unit cell). This value is very similar to the value of  $2.77 \mu_B$  reported by Chi *et al.*<sup>6</sup>

Figure 2(a) presents the magnetization isotherms  $M(H)$  of  $\text{CuNMn}_3$  at selected temperatures from 125 K to 163 K with a step of 2 K or 1 K. These  $M-H$  curves were measured after the sample was cooled down to each measurement temperature from 250 K. In all  $M(H)$  curves, the magnetization increases gradually as the field increases and no obvious jump-like or kink-like feature was observed. Separately, a very weak magnetic hysteresis was observed in the  $M(H)$  isotherms measured in an ascending/descending field cycle at 140 K and 142 K. It is worth to note that the magnetic hysteresis could be very strong in other antiperovskite compounds (e.g.,  $\text{SnCMn}_3$  and  $\text{GaCMn}_3$ ) showing typical first-order magnetic transitions.<sup>12,20</sup> The  $M(H)$  curves in Fig. 2(a) were replotted in Fig. 2(b) as  $M^2-H/M$ , i.e., the Arrott plots. It is evident that the slope is positive in each  $M^2-H/M$  curves, similar to the result reported recently by Yin *et al.*<sup>21</sup> According to the Banerjee criterion,<sup>22</sup> the positive slope of the  $M^2-H/M$  curve is usually a signal for the second-order transition.

Based on the  $M-H$  curves presented in Fig. 2(a), the magnetic entropy change can be evaluated using the Maxwell equation,<sup>20</sup>

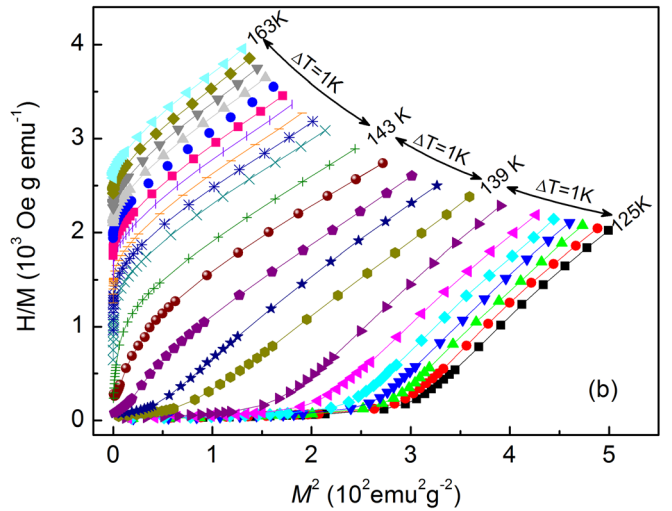
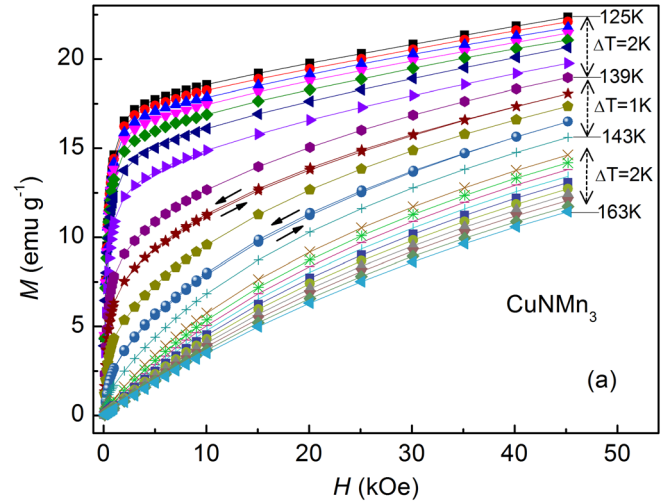


FIG. 2. (a) The initial isothermal magnetization measured around  $T_c$ . For 140 K and 142 K, both the ascending- and descending-field data are shown, otherwise only the ascending-field data is plotted. Temperature step is either 1 K or 2 K as marked. (b) Arrott plots ( $M^2$  vs  $H/M$ ) transformed from the  $M(H)$  data with ascending field cycle only.

$$\begin{aligned} \Delta S_M(T, H) &= S_M(T, H) - S_M(T, 0) \\ &= \int_0^H \left( \frac{\partial S}{\partial M} \right)_T dH = \int_0^H \left( \frac{\partial M}{\partial T} \right)_H dH. \end{aligned} \quad (1)$$

In the case of magnetization measurements at small discrete field and temperature intervals,  $\Delta S_M$  can be approximated as<sup>20</sup>

$$\left| \Delta S_M \left( \frac{T_i + T_{i+1}}{2} \right) \right| = \sum \left[ \frac{(M_i - M_{i+1})_{H_i}}{T_{i+1} - T_i} \right] \Delta H_i, \quad (2)$$

where  $M_i$  and  $M_{i+1}$  are the experimental data of the magnetization at  $T_i$  and  $T_{i+1}$ , respectively, under the same magnetic field. Fig. 3 shows the thermal variation of the magnetic entropy change  $-\Delta S_M$  under different ranges of magnetic field up to  $\Delta H = 45 \text{ kOe}$ . Under each  $\Delta H$ ,  $-\Delta S_M$  reaches the maximum value,  $-\Delta S_M^{\text{max}}$ , at 141 K. The value of  $-\Delta S_M^{\text{max}}$  is  $3.49 \text{ J/kg K}$  and  $6.38 \text{ J/kg K}$  for the field change of  $\Delta H = 20 \text{ kOe}$  and  $45 \text{ kOe}$ , respectively. From the product of

$-\Delta S_M^{\max}$  and the full width at half maximum of the  $-\Delta S_M(T)$  peak height,<sup>14</sup> the relative cooling power is estimated to be 21.29 J/kg and 39.6 J/kg for  $\Delta H=20$  kOe and 45 kOe, respectively.

For a typical first-order magnetic transition, the  $\Delta S_M$  peak should broaden asymmetrically with increasing field due to the field-induced metamagnetic transition.<sup>23</sup> Such an effect was observed in  $\text{SnCMn}_3$  associated with a first-order magnetic transition,<sup>20</sup> while absent in  $\text{AlCMn}_3$  and  $\text{GaC}_{0.78}\text{Mn}_3$  where the MCE is attributed to the second-order FM transition.<sup>14,24</sup> The  $-\Delta S_M$  peak of  $\text{CuNMn}_3$  does not show a clear asymmetric broadening as the field increases, which coincides with barely visible field-induced metamagnetic transition in the  $M$ - $H$  isothermals as shown in Fig. 2(a). The  $H^{2/3}$  dependence of  $-\Delta S_M^{\max}$  is displayed in the inset of Fig. 3. The linear fit to the data demonstrates clearly that the relationship  $-\Delta S_M^{\max} \sim H^{2/3}$  is valid around  $T_C$ . It is not surprising since magnetic properties at  $T_C$  behave as a continuous one. Actually, such a  $H^{2/3}$  law initially proposed for the second-order FM transition in the framework of the mean field theory was found to hold for the first-order magnetic transitions in  $\text{LaFe}_{11.6}\text{Si}_{1.4}$  and  $\text{LaFe}_{11.6}\text{Si}_{1.4}\text{H}_{1.6}$ .<sup>25</sup>

For the magnetic field change of  $\Delta H=45$  kOe (or 50 kOe), the magnetic entropy change at  $T_c$  in  $\text{CuNMn}_3$  (6.38 J/kg K at 141 K) is less than the values associated with the first-order transition in  $\text{SnCMn}_3$  (16.84 J/kg K at 279 K)<sup>20</sup> and  $\text{GaCMn}_3$  (13 J/kg K at 150 K),<sup>12</sup> but larger than those observed around the second-order FM transitions in  $\text{AlCMn}_3$  (3.28 J/kg K at 287 K),<sup>14</sup>  $\text{GaC}_{0.78}\text{Mn}_3$  (3.7 J/kg K at 295 K),<sup>24</sup> and  $\text{GaCMn}_3$  (4.19 J/kg K at 250 K).<sup>13</sup> According to Eq. (1), large MCE requests strong temperature and field dependences of the magnetization nearby the magnetic transition. However, the antiperovskite manganese nitrides usually have an antiferromagnetic (AFM) ground state.<sup>26</sup> The magnetization change with temperature and magnetic field at a PM-AFM transition is not as large as at a PM-FM transition. Probably due to this reason, the MCE has been less concerned in the antiperovskite manganese nitrides than in

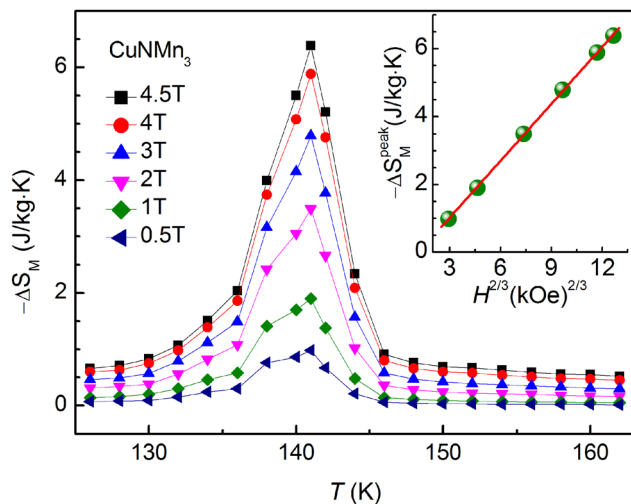


FIG. 3. Magnetic entropy change  $-\Delta S_M$  of  $\text{CuNMn}_3$  for with the field change  $\Delta H$  varying from 5 kOe and 45 kOe. Inset shows the maximum magnetic entropy change  $-\Delta S_M^{\max}$  plotted as a function of  $H^{2/3}$  along with the linear fitting (solid line).

carbides.<sup>27</sup> In fact, a FM state or FM transition can be arrived in the antiperovskite manganese nitrides by element chemical doping, even with a very small amount of dopants.<sup>28</sup> Therefore, the observation of relatively large magnetic entropy change in  $\text{CuNMn}_3$  may encourage further search for new MCE materials in the chemically doped antiperovskite manganese nitrides.

The above results suggest a continuous-like transition at  $T_C$ , which conflicts somewhat with the structural transition that usually characterizes a first-order transition. To better understand the transition at  $T_C$ , the specific heat for  $\text{CuNMn}_3$  was measured through the thermal-relaxation calorimeter equipped in QD PPMS. As shown in Fig. 4, a large peak can be seen around  $T_C$ , which is usually a hallmark of a first-order phase transition. As shown in the inset of Fig. 4, the low-temperature data, plotted as  $C(T)/T$  vs.  $T^2$ , can be well fitted linearly by using the expression,  $C(T)/T = \gamma + \beta T^2$ , where  $\gamma$  (the Sommerfeld constant) represents the electronic contribution, the second term is the lattice contribution according to the Debye approximation.<sup>29</sup> The fitted values of  $\gamma$ ,  $\beta$  are equal to 35 mJ/mol  $\text{K}^2$ , and 0.119 mJ/mol  $\text{K}^4$ , respectively. The large  $\gamma$  value indicates a large electronic density of state at the Fermi surface. By taking the formula,  $\Theta_D = (n \times 1.944 \times 10^6 / \beta)^{1/3}$ , where  $n$  is the number of atoms in a unit cell, the Debye temperature  $\Theta_D$  is estimated to be 439 K.

For heat capacity measurement in a QD PPMS, the sample is pasted with conductive grease on a platform. Experimentally, after stabilization at the initial temperature  $T_i$ , the sample/platform assembly is heated by a constant power and lasted for a period of time,  $t_0$ .<sup>30</sup> Then the power is shut off and the sample/platform assembly cools down. The temperature of the platform is monitored throughout the measurement and the temperature-time relaxation curves during both heating and cooling processes are recorded. Fig. 5(a) displays the derivatives of the relaxation curves around  $T_c$  for  $\text{CuNMn}_3$ . A broad kink showing a reduced  $dT/dt$  is clearly seen in both heating and cooling curves when  $T_i$  (e.g., 141 K and 143 K) is close to  $T_c$ , indicating the presence of the latent heat, a signature of the first-order transition.<sup>31,32</sup> As  $T_i$  departs from  $T_c$ , the kink damps out. Finally,

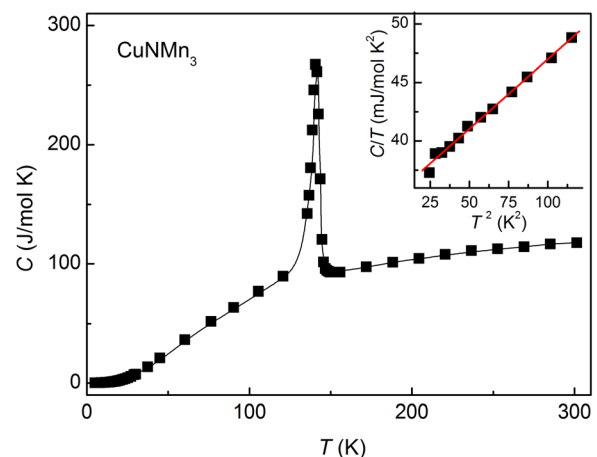


FIG. 4. Specific heat  $C(T)$  of  $\text{CuNMn}_3$ . Inset shows a linear fit to the  $C(T)/T$  vs.  $T^2$  curve at low temperatures.

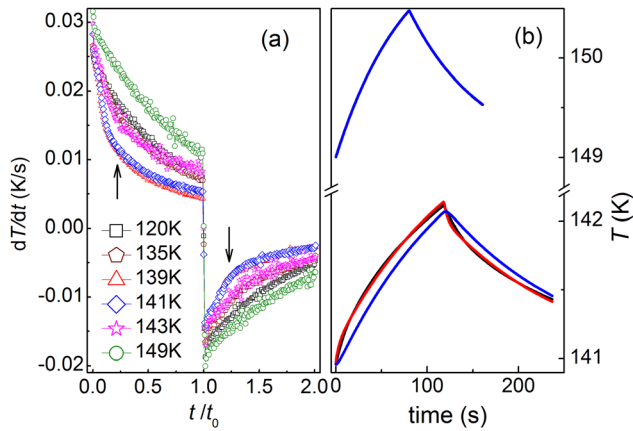


FIG. 5. (a) The derivatives of temperature-time relaxation curves recorded around  $T_c$  during the specific heat measurement for CuNMn<sub>3</sub>. The arrows indicate a reduction of  $dT/dt$ . (b) Temperature-time relaxation curves with initial temperatures of  $T_i = 141$  K and 149 K, along with the two- $\tau$  model fitting (red lines). Also shown are the calculated relaxation curves (blue lines) for the sample by using the fitting results.

it disappears when  $T_i$  (e.g.,  $T_i = 149$  K) is well above  $T_c$ , which means the temperature changes monotonically and the latent heat is no longer presented. Usually, for a typical first order phase transition,<sup>32–34</sup> a plateau- or shoulder-like structure can be expected in the temperature-time relaxation curves around  $T_c$  due to the existence of latent heat. However, as shown in Fig. 5(b), it is hard to see any anomalies in the temperature-time curve with  $T_i = 141$  K which shows the most remarkable reduction of  $dT/dt$  though. This suggests the transition under discussion is weakly first-order in nature. According to the mean field theory, the free energy in a magnetic field can be expanded as a function of magnetic field. The Banerjee criterion that ignores the higher-order terms in the free energy expansion works effectively for distinguishing the typical first-order transition from the continuous one.<sup>35</sup> For a weakly first-order transition, however, the higher-order terms in the free energy expansion are no longer ignorable and thus it is difficult for the Banerjee criterion to correctly determine the order of the transition.<sup>35,36</sup> Practically, the “S-like” shape exhibited in some  $M^2-H/M$  curves in the vicinity of  $T_c$  may give a hint of the weakly first-order magnetic transition,<sup>36</sup> though the slope is always positive.

Routinely, the software of the QD PPMS system fits the temperature-time relaxation curves with the sum of two exponentials (the so-called two- $\tau$  model).<sup>30</sup> The fitting parameters are then used to calculate the specific heat for the sample. This method assuming the heat capacity is invariable within a thermal relaxation works well when there is no phase transition or the transition is continuous.<sup>30</sup> However, it fails for a first-order phase transition because the existence of latent heat distorts the slopes of the relaxation curves. Obviously, as shown in Fig. 5(b), the two- $\tau$  model does not fit the relaxation curves around  $T_c$ , e.g., at  $T_i = 141$  K. Here, we note that the bad fitting by the two- $\tau$  model to the temperature-time curve around  $T_c$  is not due to a poorly experimental setting up since a good fitting is observed when  $T_i$  locates outside of the transition region (e.g.,  $T_i = 149$  K).<sup>30,37</sup>

The specific heat crossing a first-order transition is naturally underestimated by taking the two- $\tau$  model analysis because this model determines a single  $C(T)$  value by fitting the whole relaxation curve.<sup>30,37</sup> As proposed by Lashley *et al.*, it is more appropriate to estimate the sharp peak in the specific heat by analyzing “point-by-point” the time dependence of the relaxation.<sup>30</sup> Following this method, the  $C(T)$  traces for each thermal relaxation around  $T_c$  were calculated. For clarity purpose, only the  $C(T)$  calculated from heating branch was plotted in Fig. 6 for CuNMn<sub>3</sub>. The peak value of each  $C(T)$  trace should reflect the true capacity which is greater than that derived by the standard curve fitting using the two- $\tau$  model.<sup>37</sup> The difference between the data determined by the two methods is more evidenced around  $T_c$  than away from  $T_c$ . The specific heat change due to phase transition,  $\Delta C(T)$ , is estimated by subtracting a polynomial-function background from  $C(T)$ . And then the entropy change around  $T_c$  can be calculated by taking the expression,  $\Delta S = \int (\Delta C(T)/T)dT$ . The estimated entropy changes based on the  $C(T)$  data derived from both the two- $\tau$  model and “point-by-point” method are plotted in the inset of Fig. 6. A sharp jump of  $\Delta S$  at  $T_c$  is observed, which indicates again the transition is of first order. The  $\Delta S$  value calculated from the  $C(T)$  data determined by the “point-by-point” method is about 14.9 J/mole K.

The adiabatic temperature change ( $\Delta T_{ad}$ ) induced by an external magnetic field can be estimated by using the relation  $\Delta T_{ad} = -\Delta S_M(T, H) \times T/C_p(T, H=0)$ , where  $C_p(T, H=0)$  is the zero-field specific heat.<sup>14</sup> Under 45 kOe, the value of  $\Delta T_{ad}$  at  $T_c$  ( $\sim 141$  K) is around 0.8 K which is much smaller than the value of  $\sim 3$  K for GaCMn<sub>3</sub> associated with the first-order AFM-FM transition.<sup>15</sup> According to Ref. 38, the magnitude of  $\Delta T_{ad}$  depends on the specific heat value and how fast the magnetization changes under the external magnetic field. So, the small  $\Delta T_{ad}$  in CuNMn<sub>3</sub> is due to the high peak of the specific heat at  $T_c$ , as well as the fact that the

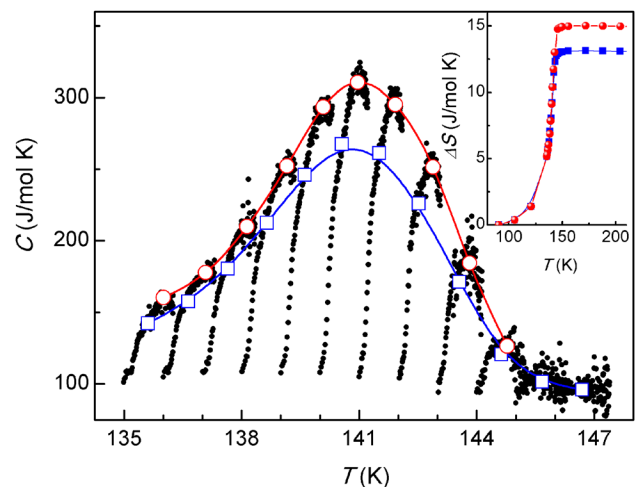


FIG. 6. Specific heat data of CuNMn<sub>3</sub> around  $T_c$ . The solid circles (black) are the data derived from the “point-by-point” analysis of the heating branches of the temperature-time relaxations. The peak value for each  $C(T)$  trace is highlighted by the open circles (red). Also shown is the data derived from the standard two- $\tau$  fitting (open squares in blue). Solid lines are the guide to the eyes.

transition at  $T_C$  in  $\text{CuNMn}_3$  is weakly first-order which does not yield a sharp magnetization change in magnetic field.

#### IV. CONCLUSION

In conclusion, the large MCE at  $T_C$  was observed in  $\text{CuNMn}_3$  with the entropy change of 3.49 J/kg K and 6.38 J/kg K for field change of  $\Delta H = 20$  kOe and 45 kOe, respectively. The detailed analysis of the temperature-time relaxation of specific heat data suggests the PM-FIM transition in  $\text{CuNMn}_3$  is weakly first-order in nature, though the isothermal magnetization, Arrott plots and MCE around  $T_C$  behave as if the transition is continuous. The present result suggests that large MCE can be expected in properly doped antiperovskite manganese nitrides.

#### ACKNOWLEDGMENTS

This work was supported by the National Key Basic Research under Contract Nos. 2011CBA00111, the National Natural Science Foundation of China under Contract Nos. 51322105, 11174295, 51301167, 51171177, 91222109, and 51371005, and the Foundation of Hefei Center for physical science and technology under Contract No. 2012FXCX007.

- <sup>1</sup>P. Tong, B. S. Wang, and Y. P. Sun, *Chin. Phys. B* **22**, 067501 (2013).
- <sup>2</sup>K. Takenaka and H. Takagi, *Appl. Phys. Lett.* **87**, 261902 (2005).
- <sup>3</sup>R. J. Huang, L. F. Li, F. S. Cai, X. D. Xu, and L. H. Qian, *Appl. Phys. Lett.* **93**, 081902 (2008).
- <sup>4</sup>X. Y. Song, Z. H. Sun, Q. Z. Huang, M. Rettenmayr, X. M. Liu, M. Seyring, G. N. Li, G. H. Rao, and F. X. Yin, *Adv. Mater.* **23**, 4690 (2011).
- <sup>5</sup>C. Wang, L. Chu, Q. Yao, Y. Sun, M. Wu, L. Ding, J. Yan, Y. Na, W. Tang, G. Li, Q. Huang, and J. Lynn, *Phys. Rev. B* **85**, 220103(R) (2012).
- <sup>6</sup>E. O. Chi, W. S. Kim, and N. H. Hur, *Solid State Commun.* **120**, 307 (2001).
- <sup>7</sup>L. Ding, C. Wang, L. H. Chu, J. Yan, Y. Y. Na, Q. Z. Huang, and X. L. Chen, *Appl. Phys. Lett.* **99**, 251905 (2011).
- <sup>8</sup>M. Hadano, A. Ozawa, K. Takenaka, N. Kaneko, T. Oe, and C. Urano, *J. Appl. Phys.* **111**, 07E120 (2012).
- <sup>9</sup>K. Kamishima, T. Goto, H. Nakagawa, N. Miura, M. Ohashi, N. Mori, T. Sasaki, and T. Kanomata, *Phys. Rev. B* **63**, 024426 (2000).
- <sup>10</sup>Y. B. Li, W. F. Li, W. J. Feng, Y. Q. Zhang, and Z. D. Zhang, *Phys. Rev. B* **72**, 024411 (2005).
- <sup>11</sup>B. S. Wang, P. Tong, Y. P. Sun, L. J. Li, W. Tang, W. J. Lu, X. B. Zhu, Z. R. Yang, and W. H. Song, *Appl. Phys. Lett.* **95**, 222509 (2009).

- <sup>12</sup>M.-H. Yu, L. H. Lewis, and A. R. Moodenbaugh, *J. Appl. Phys.* **93**, 10128 (2003).
- <sup>13</sup>B. S. Wang, P. Tong, Y. P. Sun, X. B. Zhu, X. Luo, G. Li, W. H. Song, Z. R. Yang, and J. M. Dai, *J. Appl. Phys.* **105**, 083907 (2009).
- <sup>14</sup>B. S. Wang, J. C. Lin, P. Tong, L. Zhang, W. J. Lu, X. B. Zhu, Z. R. Yang, W. H. Song, J. M. Dai, and Y. P. Sun, *J. Appl. Phys.* **108**, 093925 (2010).
- <sup>15</sup>O. Çakır and M. Acet, *Appl. Phys. Lett.* **100**, 202404 (2012).
- <sup>16</sup>T. Shibayama and K. Takenaka, *J. Appl. Phys.* **109**, 07A928 (2011).
- <sup>17</sup>K. Takenaka, T. Hamada, T. Shibayama, and K. Asano, *J. Alloy. Compd.* **577**, S291 (2013).
- <sup>18</sup>J. C. Lin, B. S. Wang, P. Tong, S. Lin, W. J. Lu, X. B. Zhu, Z. R. Yang, W. H. Song, J. M. Dai, and Y. P. Sun, *Scr. Mater.* **65**, 452 (2011).
- <sup>19</sup>K. Takenaka, K. Asano, M. Misawa, and H. Takagi, *Appl. Phys. Lett.* **92**, 011927 (2008).
- <sup>20</sup>B. S. Wang, P. Tong, Y. P. Sun, X. Luo, X. B. Zhu, G. Li, X. D. Zhu, S. B. Zhang, Z. R. Yang, W. H. Song, and J. M. Dai, *Europhys. Lett.* **85**, 47004 (2009).
- <sup>21</sup>Y. Yin, J. C. Han, Q. Yuan, L. S. Ling, and B. Song, *J. Magn. Magn. Mater.* **346**, 203 (2013).
- <sup>22</sup>S. K. Banerjee, *Phys. Lett.* **12**, 16 (1964).
- <sup>23</sup>B. G. Shen, J. R. Sun, F. X. Hu, H. W. Zhang, and Z. H. Cheng, *Adv. Mater.* **21**, 4545 (2009).
- <sup>24</sup>M. H. Yu, L. H. Lewis, and A. R. Moodenbaugh, *J. Magn. Magn. Mater.* **299**, 317 (2006).
- <sup>25</sup>J. Lyubina, M. D. Kuz'min, K. Nenkov, O. Gutfleisch, M. Richter, D. L. Schlagel, T. A. Lograsso, and K. A. Gschneidner, *Phys. Rev. B* **83**, 012403 (2011).
- <sup>26</sup>D. Fruchart and E. F. Bertaut, *J. Phys. Soc. Jpn.* **44**, 781 (1978).
- <sup>27</sup>Y. Sun, Y.-F. Guo, Y. Tsujimoto, X. Wang, J. Li, C. I. Sathish, C. Wang, and K. Yamaura, *Adv. Condens. Matter Phys.* **2013**, 286325 (2013).
- <sup>28</sup>K. Takenaka, T. Inagaki, and H. Takagi, *Appl. Phys. Lett.* **95**, 132508 (2009).
- <sup>29</sup>P. Tong, Y. Sun, X. Zhu, and W. Song, *Phys. Rev. B* **74**, 224416 (2006).
- <sup>30</sup>J. C. Lashley, M. F. Hundley, A. Migliori, J. L. Sarrao, P. G. Pagliuso, T. W. Darling, M. Jaime, J. C. Cooley, W. L. Hults, L. Morales, D. J. Thoma, J. L. Smith, J. Boerio-Goates, B. F. Woodfield, G. R. Stewart, R. A. Fisher, and N. E. Phillips, *Cryogenics* **43**, 369 (2003).
- <sup>31</sup>C. S. Mejía, A. M. Gomes, M. S. Reis, and D. L. Rocco, *Appl. Phys. Lett.* **98**, 102515 (2011).
- <sup>32</sup>C. R. Rotundu, B. Freelon, T. R. Forrest, S. D. Wilson, P. N. Valdivia, G. Pinuellas, A. Kim, J. W. Kim, Z. Islam, E. Bourret-Courchesne, N. E. Phillips, and R. J. Birgeneau, *Phys. Rev. B* **82**, 144525 (2010).
- <sup>33</sup>C. Klingner, C. Krellner, M. Brando, C. Geibel, and F. Steglich, *New J. Phys.* **13**, 083024 (2011).
- <sup>34</sup>C. Krellner, N. Caroca-Canales, A. Jesche, H. Rosner, A. Ormeci, and C. Geibel, *Phys. Rev. B* **78**, 100504 (2008).
- <sup>35</sup>K. Morrison, A. Dupas, Y. Mudryk, V. K. Pecharsky, K. A. Gschneidner, A. D. Caplin, and L. F. Cohen, *Phys. Rev. B* **87**, 134421 (2013).
- <sup>36</sup>C. M. Bonilla, J. Herrero-Albillos, F. Bartolomé, L. M. García, M. Parra-Borderías, and V. Franco, *Phys. Rev. B* **81**, 224424 (2010).
- <sup>37</sup>V. Hardy, Y. Breard, and C. Martin, *J. Phys.: Condens Matter* **21**, 075403 (2009).
- <sup>38</sup>E. Brück, *J. Phys. D: Appl. Phys.* **38**, R381 (2005).